Impact of a Control Rod on the Heat Transfer Enhancement of a Wall Jet

S. E. Razavi, B. Vojoudi*

Faculty of Mechanical Engineering, University of Tabriz, Tabriz, Iran

ABSTRACT: Influence of a control rod on the heat transfer characteristics of an incompressible wall jet with an isothermal plate boundary condition is investigated numerically in the turbulent regime. The main issue is to find an efficient way to increase the rate of convective heat transfer in the wall jet. The rod is placed in various horizontal and vertical locations. In addition, different diameters for the rod are examined. The performance of realizable K-ϵ, standard K-ω, and shear stress transport turbulence models are compared with the experimental data to find the suitable one for the simulations. It was found that the shear stress transport model generates more accurate results than the others. The control rod with a particular diameter and location causes a noticeable enhancement in the heat transfer rate with a negligible increase in the skin friction coefficient. The results showed that the effect of the rod on the heat transfer enhancement increases with the Reynolds number. Two correlations were found as the variation of average Nusselt number and Stanton number against the Reynolds number, which could be used in designs and practices.

1- Introduction

Many industrial applications use wall jets as a heat transfer or a momentum source. Wall jets can be used for the separation control in airfoils [1]. In this case, the combination of wall jet and the surrounding air increases the momentum of the boundary layer which is threatened by separation. Additionally, by injecting a hot air wall jet over the wings, freezing can be avoided. Another application is related to the gas turbine industry in which they are used as a cooling mechanism to protect the components like combustion chambers, turbine blades, and other surfaces from overheating. Evaporation enhancement is another case in which the wall jets play an important role. Some other applications of the wall jets are electronic cooling, heat exchangers, air conditioning, papers and food drying.

The transition of the wall jet flow has been examined by Hsiao and Sheu [2]. According to their results, transition depends extensively on the Reynolds (Re) number and Re number=750 is the critical one for this phenomena. Turkyilmazoglu [3] studied the effect of velocity slip and temperature jump in the laminar wall jet with a permeable plate analytically. The results show that the classical self-similar solution can be used in this problem too. Velocity slip reduces the momentum and thermal boundary layer thickness and increases the heat transfer rate from the plate. AbdulNour et al. [4] conducted an experimental study on the wall jet and indicated the temperature profiles in the thermal sublayer.

Their results are very useful for the validation of numerical studies. Several experimental studies have been carried out on the effect of wall roughness on the wall jet flow [5,6]. The results showed that the rough wall increases the decay rate of maximum velocity, skin friction coefficient, inner layer thickness, and the maximum value of turbulence intensity. Pour and Nassab [7] investigated the effect of suction and blowing on the convective heat transfer of nanofluids over a 2 Dimensional (2D) backward-facing step. According to their results, the Nusselt (Nu) number and friction coefficient increase by the volume fraction. Also, Ag has been found as the best nano-particle for heat transfer enhancement in this study. Rathore and Das [8] engaged four turbulence models to simulate the wall jet and offset jets. They compared these models with each other and with experimental results available in the literature. They reported that the Shear Stress Transport (SST) and the low-Reynolds number K-□ models have shown better agreement with the experimental data. Kumar [9] compared the flow characteristics of a dual jet (combination of a wall jet and an offset jet) with a single offset jet numerically. In the dual jet, deflection of the offset jet enhances near the impinging wall due to the presence of wall jet and as a result, it collides with the wall jet intensively. This intensity decreases with the increase of the offset ratio. Correlations for the reattachment, merge, and combined points have been found in this study. Hnaien et.al [10] investigated the effect of wall inclination on the heat transfer characteristics of a dual jet numerically. According to their results, the heat transfer rate increases for the low wall inclination, high Reynolds numbers, and constant heat

*Corresponding author's email: behnamvojodi@yahoo.com

flux boundary condition. Direct numerical simulation of a turbulent and isothermal wall jet flow was performed by Naqavi et al. [11]. They reported the temperature profiles and turbulence characteristics meticulously.

Mochizuki et al. [12] studied the turbulent wall jet flow with the Large Eddy-Break-Up (LEBU) device experimentally. The LEBU was placed in different distances from the wall, and the profiles of velocity, Reynolds shear stress, and wall shear stress were depicted under its influence. The shear layer thickness and the Reynolds shear stress decrease because of the LEBU, and the wall shear stress reduces when it is in the outer layer. A numerical and experimental study has been done on the effect of V-shape ribs on the heat transfer characteristics of an impinging jet by Chen et al. [13]. They found that the Nusselt Number of the plate with V-ribs is higher than the smooth plate. Gu et al. [14] used Large Eddy Simulation (LES) for studying the effect of rib and perturbation on the thermal and fluid flow features over a plate. According to their results, perturbation replaces the hot flow near the wall with the center flow and because of that the Nusselt number increases and the reattachment length decreases. The influence of different ribs (concave and V-shape) arrangements on the heat transfer rate in an impinging jet has been investigated by Jing et.al [15]. The study has been done in the turbulent regime numerically. They found that the arrangement is more efficient than the shape of the ribs, and the dense protrusion arrangement acts better in increasing the heat transfer rate, especially in high Reynolds numbers.

The main goal of this numerical work is to find an efficient way to increase the rate of convective heat transfer in an incompressible wall jet with an isothermal boundary condition at the plate. For this purpose, a control rod with various diameters is placed in front of the jet's nozzle in different vertical and horizontal locations. The study is conducted for different Reynolds numbers in the turbulent regime ($2000 \leq Re \leq 13000$). It should be noted that beyond Re number=13000, the flow (air) becomes compressible in this study (Mach number gets larger than 0.3). Therefore, this would be the limiting Re number. The optimum location and diameter of the rod which causes the Nusselt number enhancement are specified.

2- Mathematical Formulation

Reynolds-Average Navier-Stokes (RANS) equations are used in the modeling of an incompressible and unsteady wall jet flow, which are mentioned as following. Presence of the rod in front of the jet flow causes unsteadiness due to the vortex shedding. Realizable K-□ [16], standard K-ω [17], and the SST [18,19] turbulence models are employed for solving the Reynolds stress terms. These models are based on the Boussinesq hypothesis.

$$\frac{\partial \overline{u_i}}{\partial x_i} = 0 \tag{1}$$

$$\frac{\partial \overline{u_i}}{\partial t} + \overline{u_j}\frac{\partial \overline{u_i}}{\partial x_j} = -\frac{1}{\rho}\frac{\partial \overline{P}}{\partial x_i} + \frac{\partial}{\partial x_j}[(v+v_t)(\frac{\partial \overline{u_i}}{\partial x_j}+\frac{\partial \overline{u_j}}{\partial x_i})] \tag{2}$$

$$\frac{\partial \overline{T}}{\partial t} + \overline{u_j}\frac{\partial \overline{T}}{\partial x_j} = (\alpha + \frac{v_t}{Pr_t})\frac{\partial}{\partial x_j}(\frac{\partial \overline{T}}{\partial x_j}) \tag{3}$$

where the superscript (-) shows the main part of the variables, v_t is the kinematic eddy viscosity, α is the thermal diffusivity, and Pr_t is the turbulent Prandtl number which is assumed to be 0.85 in this study.

2- 1- Parameter definition

For studying the heat transfer characteristics, two different definitions for the Nusselt number are used as follows:

Local Nusselt number [11,20]:

$$Nu = \frac{e(x)h}{k} \text{ and } Nu_x = \frac{e(x)x}{k} \tag{4, 5}$$

Average Nusselt number: $Nu_{avg} = \frac{1}{L}\int_0^L \frac{e(x)h}{k}dx \tag{6}$

where $e(x) = q(x)/(T_p - T_j)$, q(x) is the plate heat flux, T_p is the plate temperature, T_j is the jet temperature at the inlet, h is the width of the nozzle, and L is the length of the plate.

3- Solution Methodology

The governing equations are discretized by the finite volume method. Second order upwind scheme is used to discretize the convective terms in the equations. The diffusive terms are discretized by the second-order central-difference scheme and the first-order implicit scheme is used for discretizing the time derivatives. The pressure-velocity coupling is solved by the Semi-Implicit Method for Pressure-Linked Equations-Consistent (SIMPLEC) [21]. The convergence criteria for the temperature residual is 10^{-6}, and for the other variables is 10^{-5}.

3- 1- Boundary conditions

The no-slip boundary condition ($u_i = 0$) is applied to the solid walls. The turbulence intensity (I) is assumed to be 0.05, and the turbulence kinetic energy is prescribed as $K = 1.5I^2$. The main fluid is the air with constant properties. The jet temperature at the inlet is $T_j = 22°C$, the isothermal plate temperature is $T_p = 45°C$, and the rod is insulated. The Neumann boundary condition $\partial \varphi/\partial y = 0$ is imposed at the outlet boundaries, where $\varphi = u, k, T, \omega, \varepsilon$. All other boundary conditions are chosen according to the reference [8]. Fig. 1 shows the computational domain and related boundaries.

3- 2- Grid and time step independence study

The average Nusselt number (Nu_{avg}) is used as the parameter in grid and time independence studies. As a desire of K-ω models, the first near-wall grid points are placed in the viscous sublayer ($y^+ = 1$). The wall function is used for the realizable K-□ model. Fig. 2 shows the grid and time
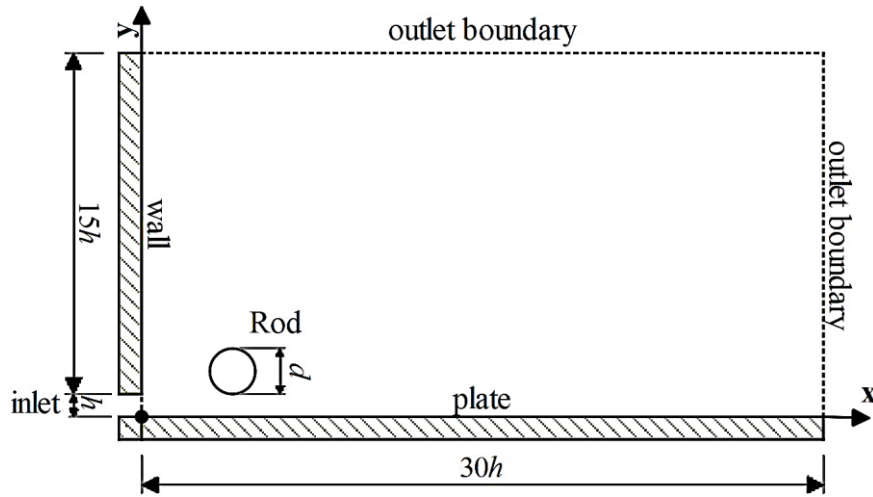
Fig. 1. Computational domain and boundaries

| (a) | (b) |
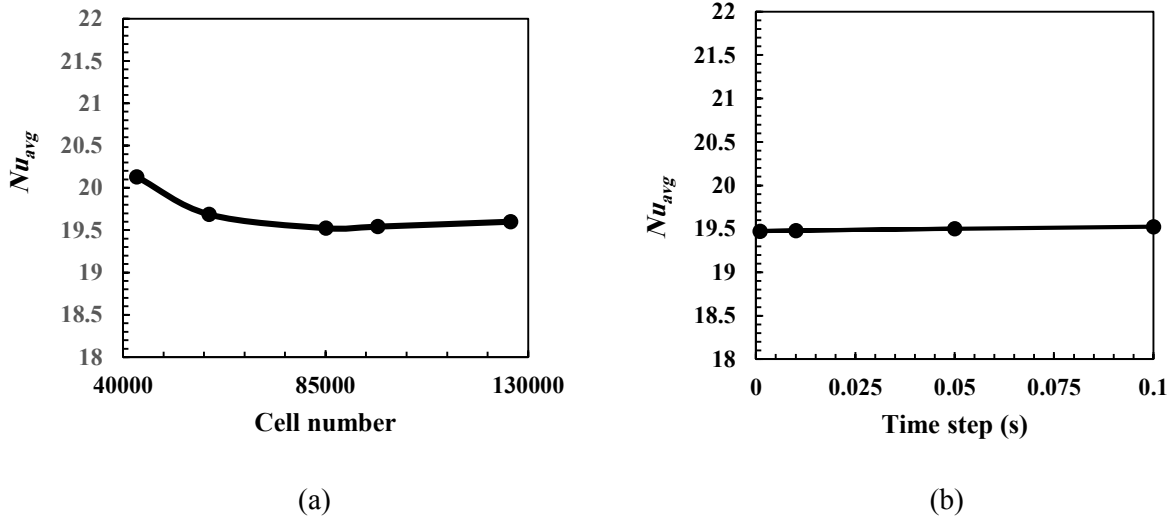
Fig. 2. (a) Grid independence study; (b) Time independence study of the wall jet with the rod

step independence studies for the turbulent wall jet with the rod (d=h/2). Based on the plot, the grid size of 85043 is the proper one. The 0.1 s is selected as the time step. The same procedure is done for the other cases (d=h/4 and h) and the suitable grid numbers are chosen. Fig. 3 shows a part of the grid which is used in computations.

3- 3- Validation of the numerical solutions

For validating the numerical schemes, three mentioned turbulence models were used to simulate a wall jet flow. The results of these models are compared with the experimental data [4,8] available in the literature to obtain the suitable turbulence model for the main problem. Fig. 4 shows the velocity profile and the local convection heat transfer coefficient of the wall jet in the self-similar region. As can be seen, the SST model has better agreement with the experimental data. Consequently, this model was selected as the applicable one for the rest of the research.

4- Results and Discussion

For finding the optimum position and diameter of the rod causing heat transfer enhancement, various horizontal locations on the plate were examined. Then three different vertical locations for the optimum x location were checked. Finally, three different diameters for the rod at the obtained optimum position were tested.

4- 1- Ideal horizontal location

Fig. 5 represents the average Nusselt number variation against various rod horizontal locations on the plate. The rod's diameter and the vertical distance from the plate are assumed to be h/2. According to the plots, In the case of x=h, the rod acts efficiently in comparison with other locations. In this position, the total heat transfer rate increases because of the enhancement in the velocity of flow under the rod (see Fig. 6) and the reduction in the thermal boundary layer thickness. As the rod goes downward, it cannot accelerate the
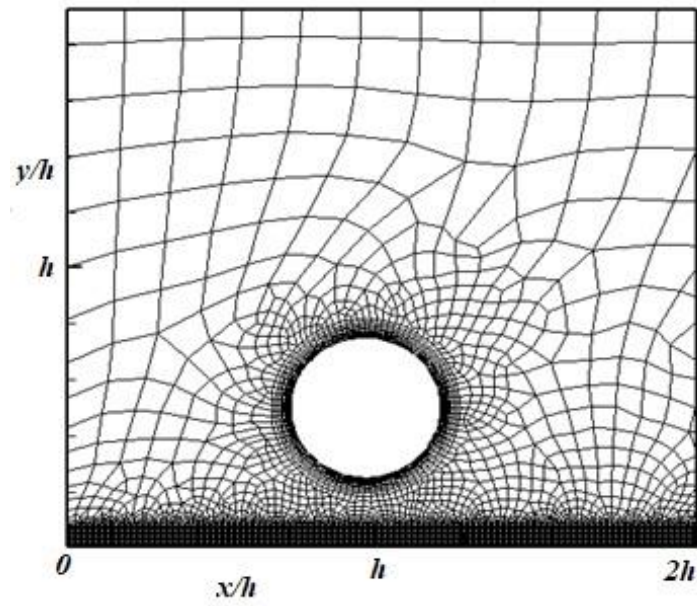
Fig. 3. Part of an enlarged grid near the rod

(a)

(b)
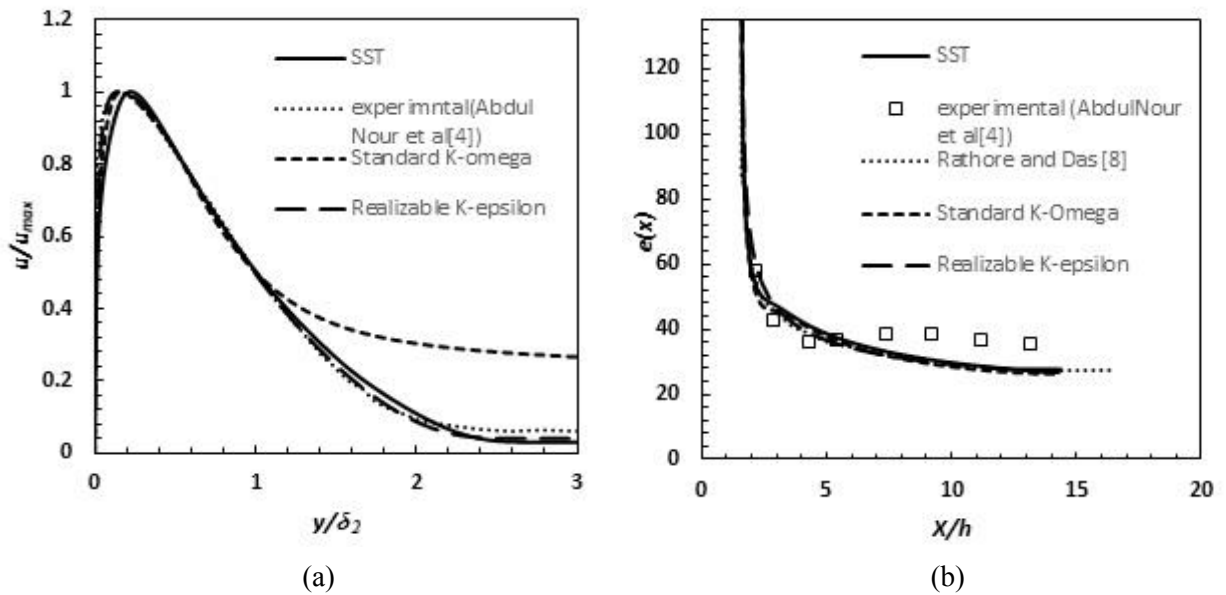
Fig. 4. Comparison of the turbulence models performance; (a) Velocity profile in the self-similar region of the wall jet; (b) Local convection heat transfer coefficient of the wall jet
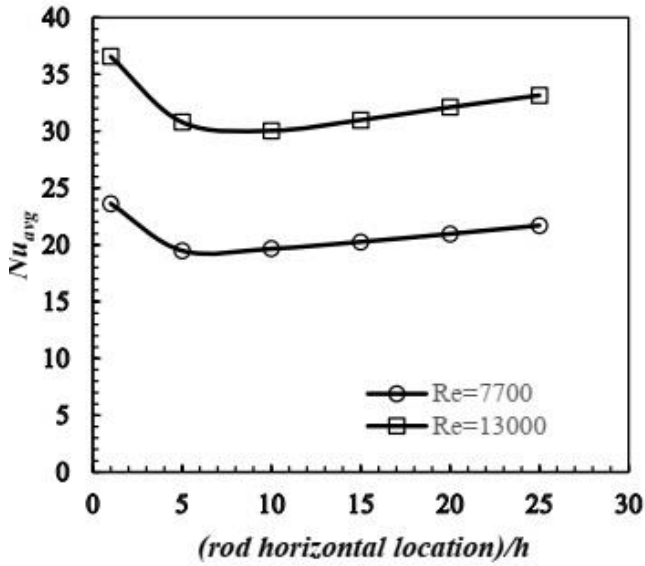
Fig. 5. Average Nusselt number variations against different rod horizontal locations on the plate
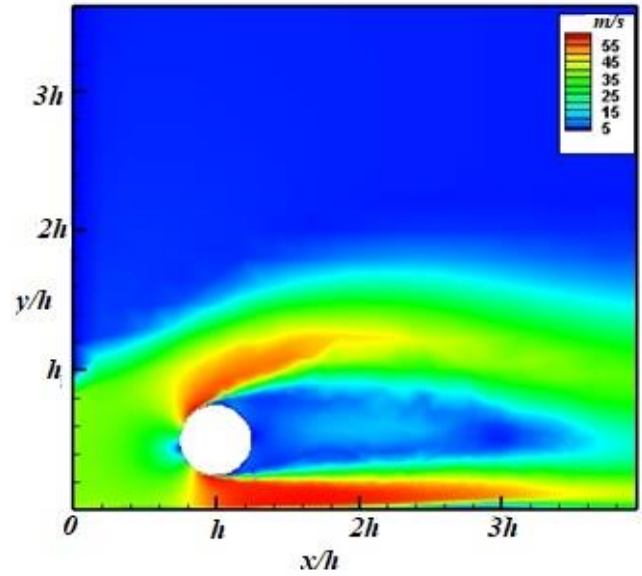
Fig. 6. Close-up of velocity contour near the rod at Re=7700
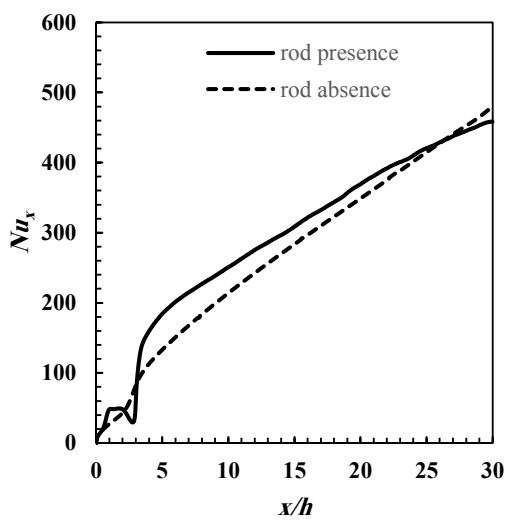
(a) *Re*=7700
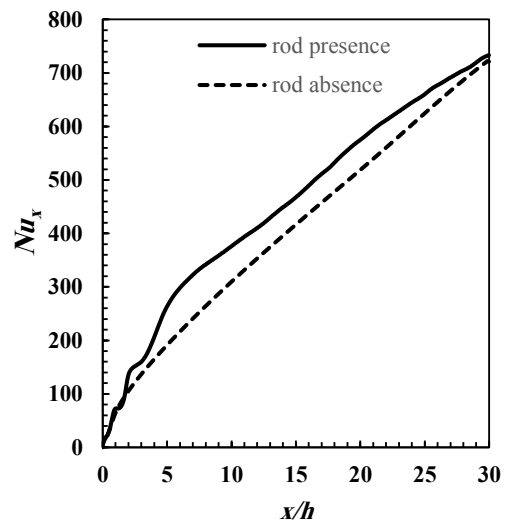
(b) *Re*=13000

Fig. 7. Local Nusselt number profiles of the wall jet with the rod (x=h, y=h/2, d=h/2)

flow efficiently because the momentum of jet flow decreases. At x=5h, the rod acts as a hinder and the flow after it has lower momentum to remove heat from the plate. For x>5h, the low flow momentum region after the rod decreases and the average Nusselt number increases. Fig. 7 depicts local Nusselt number (Nu_x) variation of the plate in the wall jet with the rod and compares it with the profile of wall jet without the rod. Based on the definition of Nu_x, its plot rises because as the flow goes downstream, the value of x increases. The plots are drawn for the rod's horizontal location at x=h against the non-dimensional distance (x/h). It can be seen that, for having a remarkable effect on the heat transfer, the rod should be placed close to the nozzle. Therefore, x=h is the optimum horizontal distance.

4- 2- Ideal vertical location

The percent of heat transfer enhancement due to the rod presence at the optimum x location (x=h) and various vertical locations is cited in Table 1 for different Reynolds numbers. The rod diameter is considered to be h/2. The average Nusselt number variation in different y locations for the rod is depicted in Fig. 8. When the rod is on the plate (y=h/4), the flow separates from the plate because of the rod presence and then attaches to it again. The heat transfer rate is very high in the reattachment point and this causes an increase in the average Nusselt number. For the case of y=h, the rod acts as a small nozzle which increases the near-wall velocity. The newly generated wall jet removes more heat from the plate due to its higher inertia. It can be concluded that in all of the

Table 1. Percent of heat transfer enhancement in different vertical locations and Reynolds numbers

Re	5000	7700	10000	13000
y=h/4	4	9	10	11
y=h/2	3	6	9	10
y=h	5	10	12	14
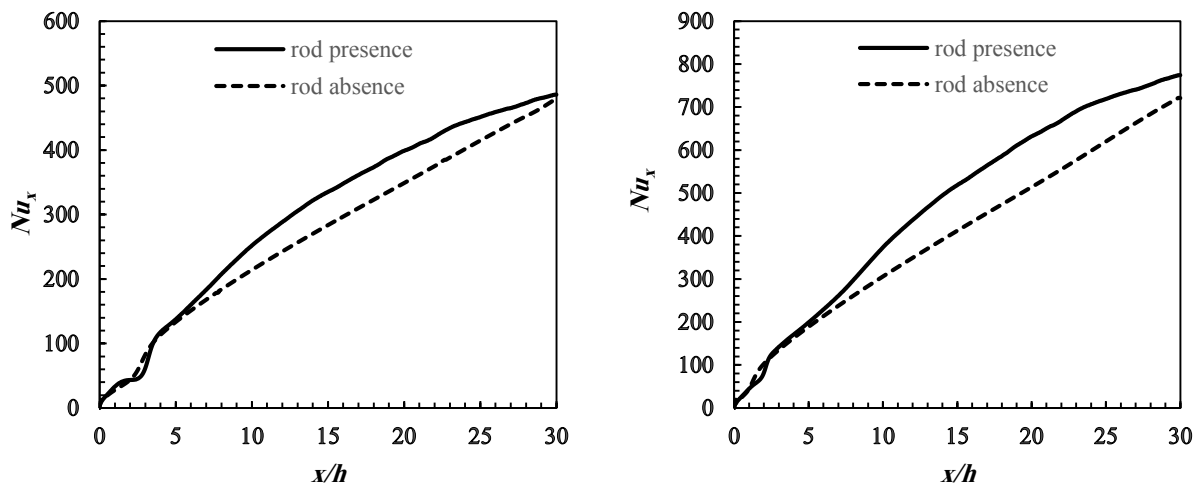
Fig. 9. Local Nusselt number variation of the wall jet with the rod (x=h, y=h, d=h/2)
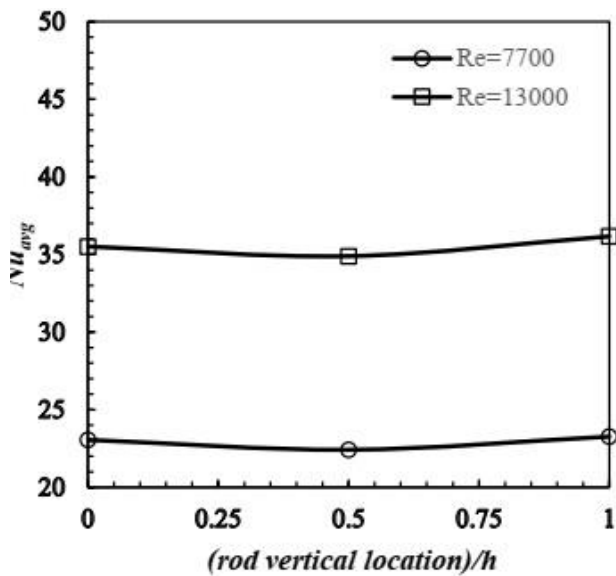
Fig. 8. Average Nusselt number variations against different vertical locations of the rod

cases the heat transfer rate increases, but more noticeable one is for y=h. Fig. 9 show the local Nusselt number plots for x=h, y=h, and d=h/2. As can be seen, the heat transfer rate of the wall jet with the rod is higher than the wall jet without the rod.

4- 3- Ideal diameter

Finally, the appropriate diameter is examined. In this case, the computations are done for x=h, y=h, and d=h/4, h/2, h. The percent of enhancement in the heat transfer rate is given in Table 2. Fig. 10 depicts the average Nusselt number distribution against different rod diameters. As the diameter size increases, the rod accelerates the flow more efficiently which causes higher enhancement in the heat transfer rate. According to the results, d=h is the suitable diameter size for increasing the convective heat transfer rate from the plate. The local Nusselt number of the wall jet with the optimized rod (x=h, y=h, d=h) is shown in Fig. 11. Fig. 12 illustrates an example of velocity contour of the wall jet with the optimized rod.

Table 2. Percent of the enhancement in the heat transfer rate due to different rod diameters and Reynolds numbers

Re	5000	7700	10000	13000
d=h/4	3	7	9	10
d=h/2	5	10	12	14
d=h	16	20	23	25
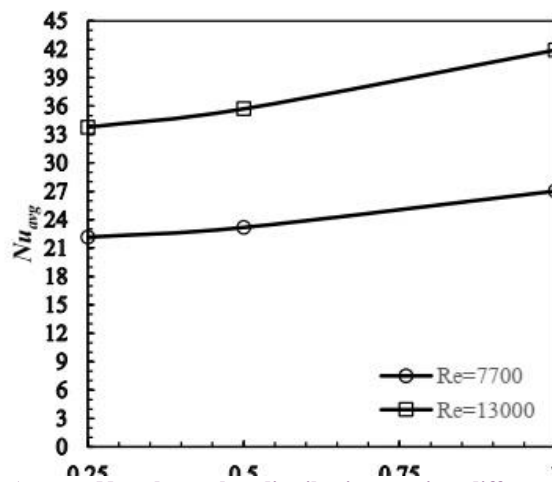
Fig. 10. Average Nusselt number distributions against different rod diameters

(a) *Re*=7700   (b) *Re*=13000
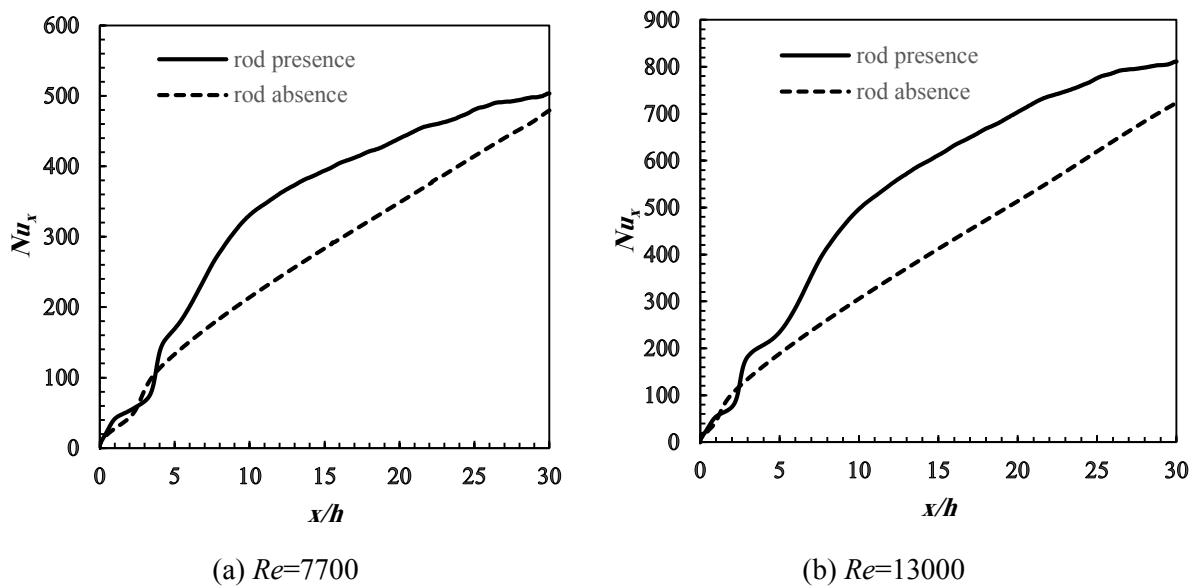
Fig. 11. Local Nusselt number variations of the wall jet with the optimized rod at different Reynolds numbers
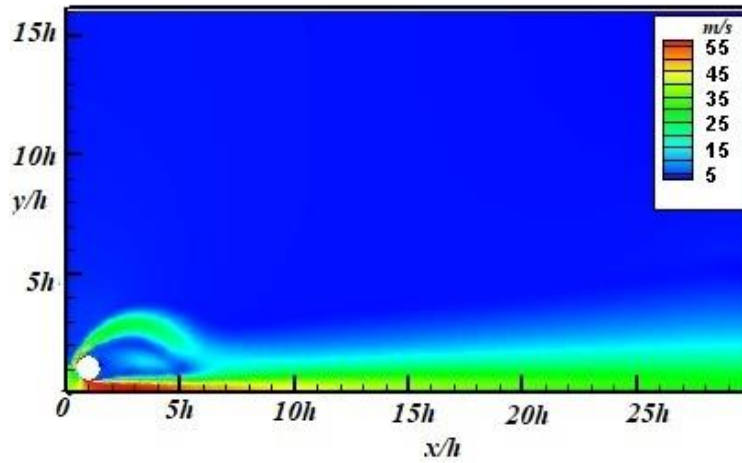
Fig. 12. Contour of velocity for the optimized case at Re=7700
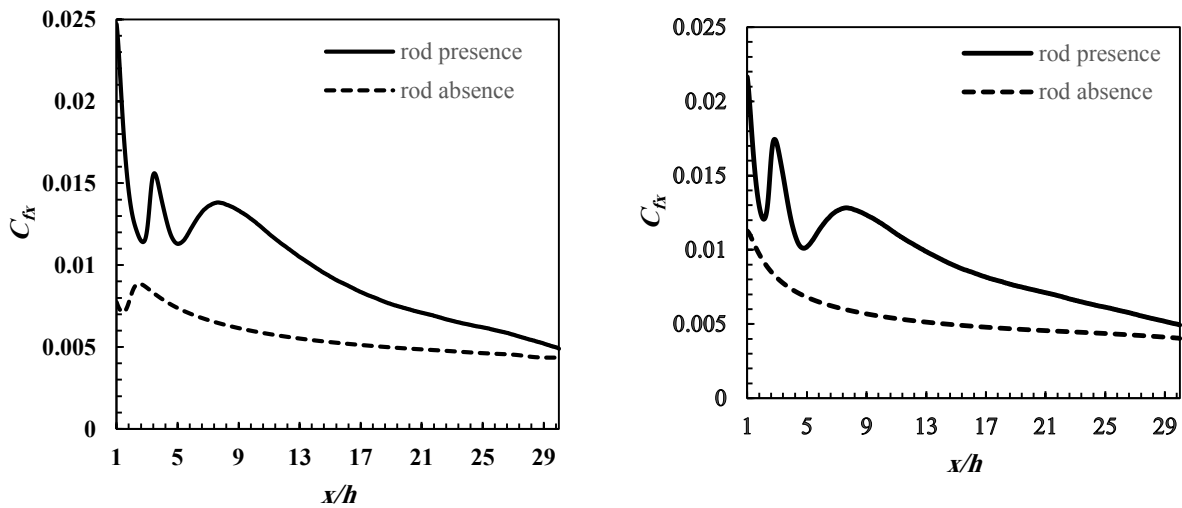
Fig. 14. Skin friction coefficient of the wall jet with the optimum rod at different Reynolds numbers
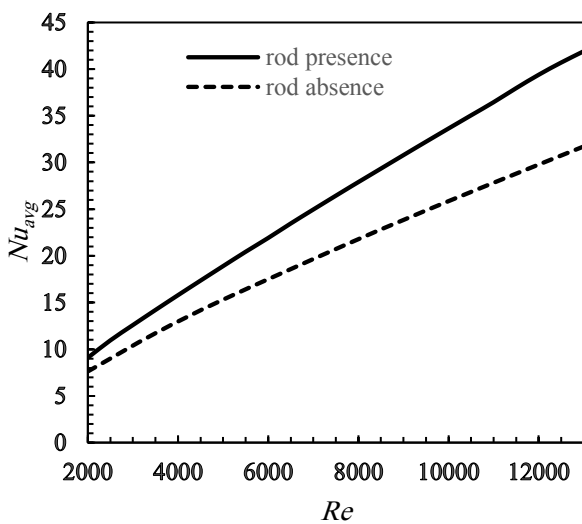
Fig. 13. Average Nusselt number variations against different vertical locations of the rod

4- 4- Correlation between the average Nusselt number and the Reynolds number

The Average Nusselt number plot against the Reynolds number for the wall jet with the optimized rod is drawn in Fig. 13. It can be identified that as the Reynolds number increases, the rod causes more enhancement in the heat transfer rate.

The following correlation for the Nu_{avg} of the wall jet with the optimized rod and the Re number is found after a large number of runs:

$$Nu_{avg} = 0.0161Re^{0.8302} \qquad (2000 \le Re \le 13000) \quad (7)$$

4- 5- Skin friction coefficient in the case of wall jet with the optimized rod

Fig. 14 illustrates the local skin friction coefficient ($C_{fx} = \tau_w / \frac{1}{2}\rho u^2$) in the region after the rod for two different Reynolds numbers. According to the plots, the difference between the C_{fx} of wall jet with the optimum rod and the wall
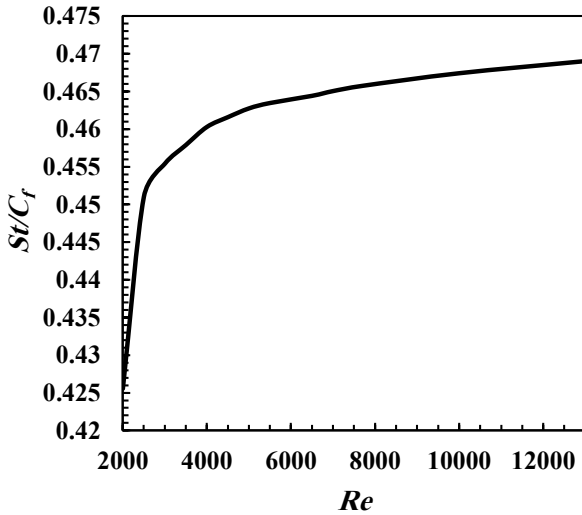
Fig. 15. Relation between St/Cf and Reynolds number for the optimum case

jet without the rod is insignificant, and as the Re number increases, this discrepancy cuts down. The fluctuations at the first part of the plot are related to the separated flow from the rod surface (see Fig. 12).

Fig. 15 shows the variation of St/C_f versus the Re number for the optimum case. This plot relates the heat transfer rate to the wall shear stress. It can be seen that as the Re number increases, the St/C_f tends to a certain value around 0.47. A correlation as the Reynolds analogy is introduced as follows:

$$\frac{St}{C_f} = -3.874 \times 10^8 \, Re^{-3.029} + 0.4661$$

(8)

$$(2000 \leq Re \leq 13000)$$

5- Conclusion

The aim of this numerical study was to enhance the convective heat transfer in a wall jet by inserting a control rod. The wall jet flow was simulated in the turbulent regime ($2000 \leq Re \leq 13000$). The SST turbulence model was selected for the simulation of the main problem. The rod was placed in different horizontal and vertical locations. In addition, various rod diameters were examined.

Based on the Nusselt number profiles, when the rod is close to the jet's nozzle it can improve the heat transfer rate. Additionally, it was revealed that a large diameter size for the rod is more efficient in the Nusselt number enhancement. According to the results, x=h, y=h, and d=h were the best index for the control rod. In this location and with this diameter size, the rod accelerates the near-wall flow and consequently, the convective heat transfer rate increases.

It was concluded that the high Reynolds numbers lead to more augmentation in the heat transfer rate. A correlation between the average Nusselt number of the wall jet with the optimized rod and the Reynolds number was introduced.

For the case of wall jet with the optimum rod, the rise of the skin friction coefficient is negligible. Another correlation between the St/C$_f$ and the Reynolds number was established. Therefore, the Reynolds analogy was fulfilled.

Nomenclature

C_f	average skin friction coefficient, $\tau_{wavg} / \frac{1}{2}\rho u^2$
C_{fx}	local skin friction coefficient, $\tau_w / \frac{1}{2}\rho u^2$
d	diameter of the rod, m
h	width of the nozzle, m
$e(x)$	local convection heat transfer coefficient, W/m^2.°C
K	turbulence kinetic energy, m^2/s^2
k	thermal conductivity, W/(m^2.°C)
L	length of the plate, m
Nu	Nusselt number, $Nu = \frac{e(x)h}{k}$
Nu_{avg}	average Nusselt number, $\frac{1}{L}\int_0^L \frac{e(x)h}{k}dx$
Nu_x	local Nusselt number, $\frac{e(x)x}{k}$
P	pressure, Pa
Pr	Prandtl number, v/α
Pr_t	turbulent Prandtl number
Re	Reynolds number, $(U_0 \, h)/v$
St	Stanton number, $Nu / RePr$
T	temperature, °C
T_p	plate temperature, °C
T_j	jet temperature, °C
t	time, s
u	velocity, m/s
u_{max}	local maximum velocity, m/s
x, y	coordinates, m

Greek

α	thermal diffusivity, $k/(\rho c_p)$
v	kinematic viscosity, m^2/s

ϵ rate of dissipation of turbulence kinetic energy, $m^2\!/s^3$

ω rate of specific dissipation, $1\!/s$

τ_w wall shear stress, Pa

δ_2 jet half width where $u = u_{max} / 2$, m

Subscripts

i, j correspond to x, y directions, respectively

References

[1] K. Javadi, M. Hajipour, Separation control using quasi-radial wall jets, aerospace science and technology, 68 (2017) 240-251.

[2] F.B. Hsiao, S.S. Sheu, Experimental studies on flow transition of a plane wall jet, The Aeronautical Journal, 100(999) (1996) 373-380.

[3] M. Turkyilmazoglu, Laminar slip wall jet of Glauert type and heat transfer, International Journal of Heat Mass Transfer, 134 (2019) 1153-1158.

[4] R.S. AbdulNour, K. Willenborg, J.J. McGrath, J.F. Foss, B.S. AbdulNour, Measurements of the convection heat transfer coefficient for a planar wall jet: uniform temperature and uniform heat flux boundary conditions, Experimental Thermal and Fluid Science, 22(3-4) (2000) 123-131.

[5] Z. Tang, D.J. Bergstrom, J.D. Bugg, A plane turbulent wall jet on a fully rough surface, International Journal of Heat and Fluid Flow, 66 (2017) 258-264.

[6] A. Shojaeizadeh, M.R. Safaei, A.A. Alrashed, M. Ghodsian, M. Geza, M.A. Abbassi, Bed roughness effects on characteristics of turbulent confined wall jets, Measurement, 122 (2018) 325-338.

[7] M. S. Pour, S. A. G. Nassab, Numerical investigation of forced laminar convection flow of nanofluids over a backward facing step under bleeding condition, Journal of Mechanics, 28(2) (2012) N7-N12.

[8] S.K. Rathore, M.K. Das, A comparative study of heat transfer characteristics of wall-bounded jets using different turbulence models, International Journal of Thermal Sciences, 89 (2015) 337-356.

[9] A. Kumar, Mean flow characteristics of a turbulent dual jet consisting of a plane wall jet and a parallel offset jet, Computers & Fluids, 114 (2015) 48-65.

[10] N. Hnaien, S. Marzouk, H.B. Aissia, J. Jay, Wall inclination effect in heat transfer characteristics of a combined wall and offset jet flow, International Journal of Heat and Fluid Flow, 64 (2017) 66-78.

[11] I.Z. Naqavi, J.C. Tyacke, P.G. Tucker, A numerical study of a plane wall jet with heat transfer, International Journal of Heat and Fluid Flow, 63 (2017) 99-107.

[12] S. Mochizuki, S. Yamada, H. Osaka, Management of a plane turbulent wall jet by the large-eddy break-up device, JSME International Journal Series B Fluids and Thermal Engineering, 49(4) (2006) 921-927.

[13] L. Chen, R.G. Brakmann, B. Weigand, J. Rodriguez, M. Crawford, R. Poser, Experimental and numerical heat transfer investigation of an impingement jet array with V-ribs on the target plate and on the impingement plate, International Journal of Heat and Fluid Flow, 68 (2017) 126-138.

[14] H. Gu, M. Yao, P. Zhao, X. Li, M. Liu, Numerical simulation of manipulated flow and heat transfer over surface-mounted rib, International Journal of Thermal Sciences, 129 (2018) 124-134.

[15] Q. Jing, D. Zhang, Y. Xie, Numerical investigations of impingement cooling performance on flat and non-flat targets with dimple/protrusion and triangular rib, International Journal of Heat and Mass Transfer, 126 (2018) 169-190.

[16] T.H. Shih, W.W. Liou, A. Shabbir, Z. Yang, J. Zhu, A new k-☐ eddy viscosity model for high reynolds number turbulent flows, Computers & Fluids, 24(3) (1995) 227-238.

[17] D.C. Wilcox, Turbulence modeling for CFD, DCW industries La Canada, CA, 1998.

[18] F.R. Menter, Improved two-equation k-turbulence models for aerodynamic flows, NASA technical memorandum, 103975(1) (1992).

[19] F.R. Menter, Review of the shear-stress transport turbulence model experience from an industrial perspective, International Journal of Computational Fluid Dynamics, 23(4) (2009) 305-316.

[20] W.H. Schwarz, B. Caswell, Some heat transfer characteristics of the two-dimensional laminar incompressible wall jet, Chemical Engineering Science, 16(3-4) (1961) 338-351.

[21] J. Van Doormaal, G.D. Raithby, Enhancements of the SIMPLE method for predicting incompressible fluid flows, Numerical heat transfer, 7(2) (1984) 147-163.